Supplementary Information

Title: Robust MRI contrast agent for specific display on the interstitial stream

Xiaohan Zhou[1,3,‡], Junwei Cheng[2,‡], Fangfei He[1,2], Zhuo Ao[1,3], Peisen Zhang[2], Jing Wang[4], Qing Li[5], Weinan Tang[1,6], Yiyan Zhou[7], Yan Liang[1,3], Yi Hou[2,], Wentao Liu[1,3,*] and Dong Han[1,3,*]*

The PAA-Gd agent injected via IVI have strong first-pass effect. The blood flow motivates the spread of agent long most arteries, veins and blood capillaries. Signal increasements are observed in organs such as heart (**Figure S1k, l**), liver (**Figure S1k, l, m**), kidneys (**Figure S1h, i, j**) and brain (**Figure S1n**), and vessel systems including jugular veins (**Figure S1l, m**), abdominal aorta (**Figure S1i, j**), postcaval vein (**Figure S1j**), iliac artery (**Figure S1j**), vena spermatica interna (**Figure S1j**) and renal veins (**FigureS1j**).

Closer insight into the histochemical staining result (**Figure S2b**) indicates little content of Gd^{3+} in the LCT via IVI. **Figure S2** displays a comparison between two groups, namely the biodistribution of Gd^{3+} at the renal cortex and hilum with a higher contrast in green to red/blue (**Figure S2k**) for the ISI group to distinguish from the IVI group. In the 20× section (**Figure S2e, f**), the LCT at renal hilum were dyed to deep green because of the high content level of local Gd^{3+}. The RGB scatter figures with data extracted from ROIs in **Figure S2e** and **Figure S2f** reveal a higher value in green channels rather than red or blue channels for the ISI group when compared to that of the IVI group. The results reveal that PAA-Gd can reveal and trace the transportation and distribution post-injection along ISI pathway, especially within the

interstitial stream and can be analysed with the semi-quantitative analysis method of CPN III staining.

The histochemical slices of the ISI group focus on the artery in kidney (**Figure S3d, e, f**) reveal that PAA-Gd agent leak little into the blood vessel as the red blood cells are not dyed to green color after CPN III stain (**Figure S3c, f**). The tunica interna of artery showed are indicated purple (**Figure S3e, f**), which implied a low leakage of agent PAA-Gd through arteries. The collagen is dyed to blue in Masson trichrome stain (**Figure S3d**) and is dyed to green after CPN III stain, indicating the contribution from PAA-Gd agent at the outer membrane of tunica externa.

According to the integrated peaks areas, ~ 97.3% of carboxyl groups in PAA were convert to amino groups after conjugating with DET, and ca. 92.7.0% of carboxyl groups were finally conjugated with DTPA.

Satisfactory colloidal stability is one of the prerequisites for exploring the biomedical applications of nanomaterials since this stability. Therefore, the colloidal stability of PAA-Gd in aqueous solution was monitored in terms of DLS. As shown in **Figure S9**, the temporal variation of the hydrodynamic size (D_h) and electrophoretic mobility of PAA-Gd in both phosphate buffered saline (PBS) and normal saline (NS) strongly supports that can prevent the aggregation of PAA-Gd under physiological conditions for at least one week.

Figure S1.

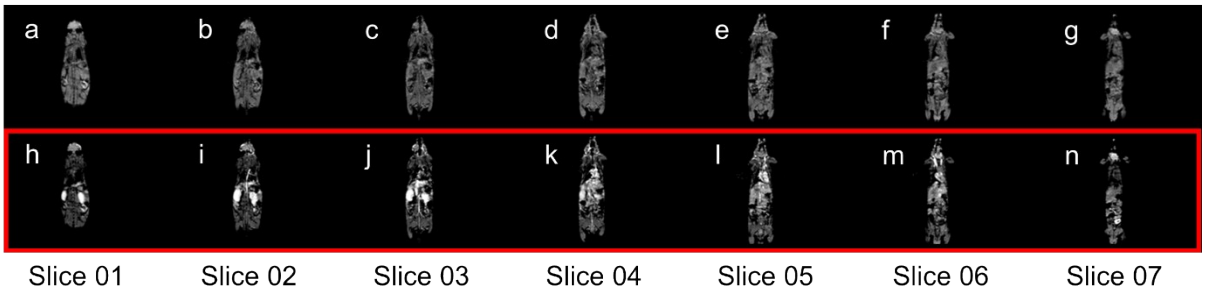

Figure S1. | The adjacent slices of DCE images after IVI. The top panel is initial time point (**a** to **g**), and the bottom panel (**h** to **n**) is the frames immediately after injection.

Figure S2

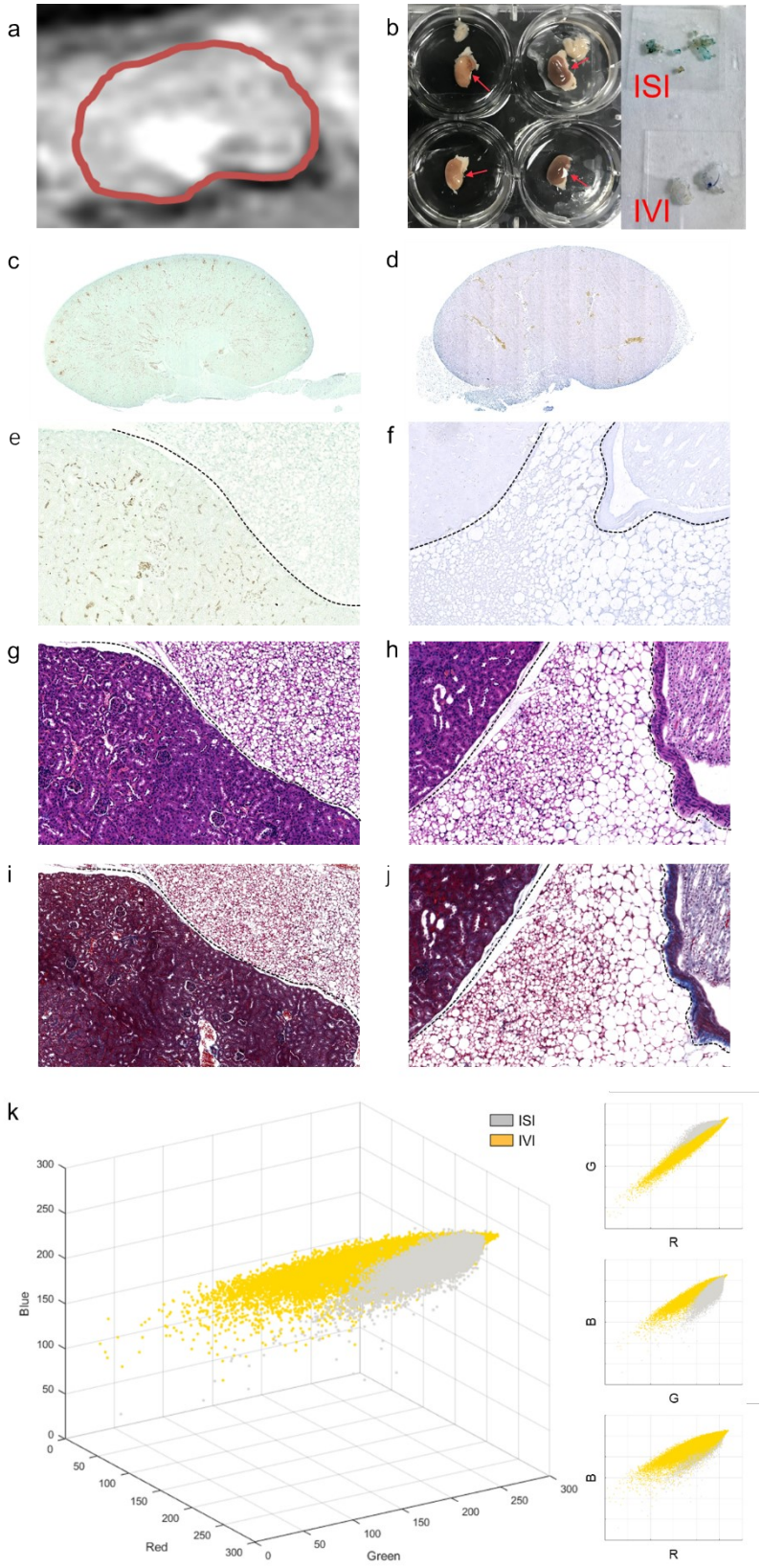

Figure S2. | Histochemical slice of the ISI group versus the IVI group. (**a**) the MRI result of the ISI group showing kidney slice. (**b**) the dissected kidney from the

ISI group and the IVI group dipped in phosphoric acid buffer solution with arrows pointing at the LCTs, which then dyed with CPN III. Form the second row to last: Left column are the histological staining slices of the ISI group stained with CPN III (**c**) and the magnified view at 20 times on the edge of renal hilus (**e**), H&E (**g**) and Masson trichrome stain (**i**) with the adjacent slices under the same field of view. Right column are the corresponding slices (**d, f, h, g**) of the IVI group. The dark dash line distinguished the LCT from parenchyma, and the LCT ROIs were selected in the third top panel according to cytoplasm deposition in H&E (**g** and **h**) and Masson trichrome stain (**i** and **j**). (**k**) the three-dimensional scatter figure of RGB (red, green, and blue ranging from 0 to 255) values in all pixels analysed in the CPN III stained sliced (grey dots for ISI, yellow dots for IVI). From the top to the bottom panels on the right column are display the projection on the green to red view, the blue to green view, and the blue to red view.

Figure. S3.

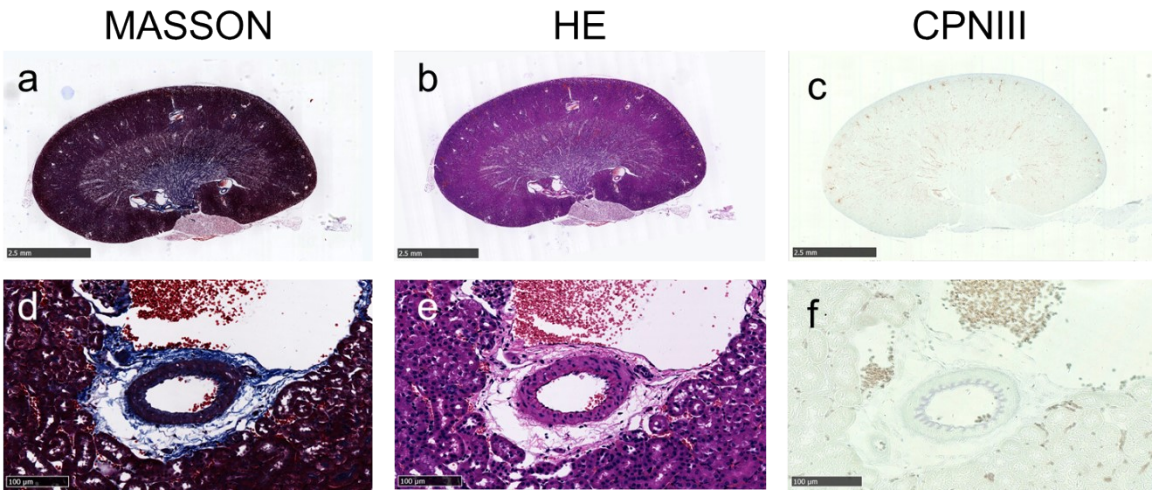

Figure S3. | The adjacent slices of histochemical dying using adjacent sections after ISI. From the left column to right are Masson trichrome stain, H&E stain, and CPN III stain.

Figure. S4.

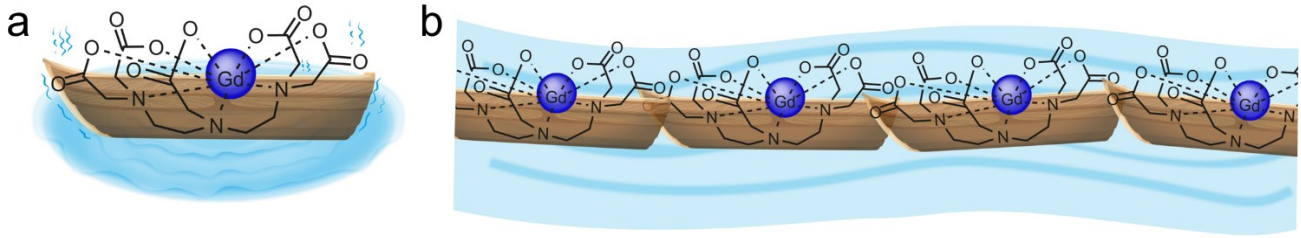

Figure S4. | A schematic illustration of the DTPA-Gd agent (**a**) compared with PAA-Gd macromolecule (**b**) linked in a long chain to ease the twiddling in the fluid.

Figure. S5.

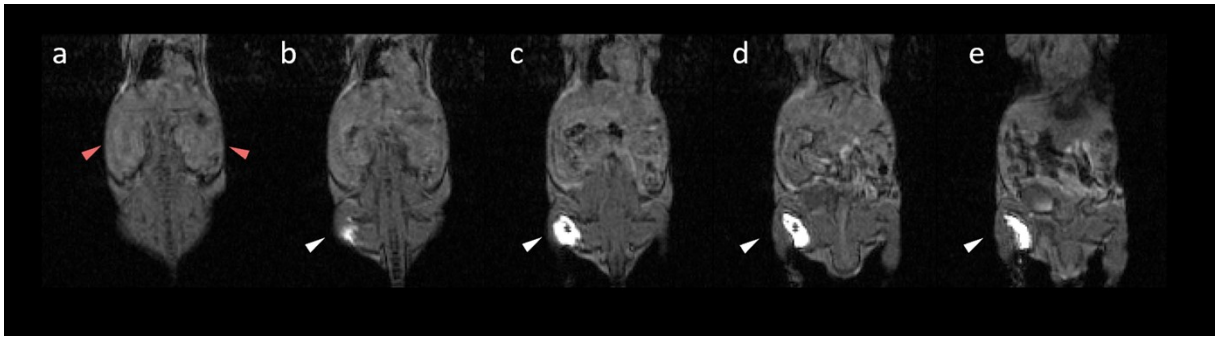

Figure S5. | The adjacent slices of DCE images 6 min after ISI with Gd-DTPA. Red arrows indicate kidneys and white arrows point at injection sites.

Figure. S6.

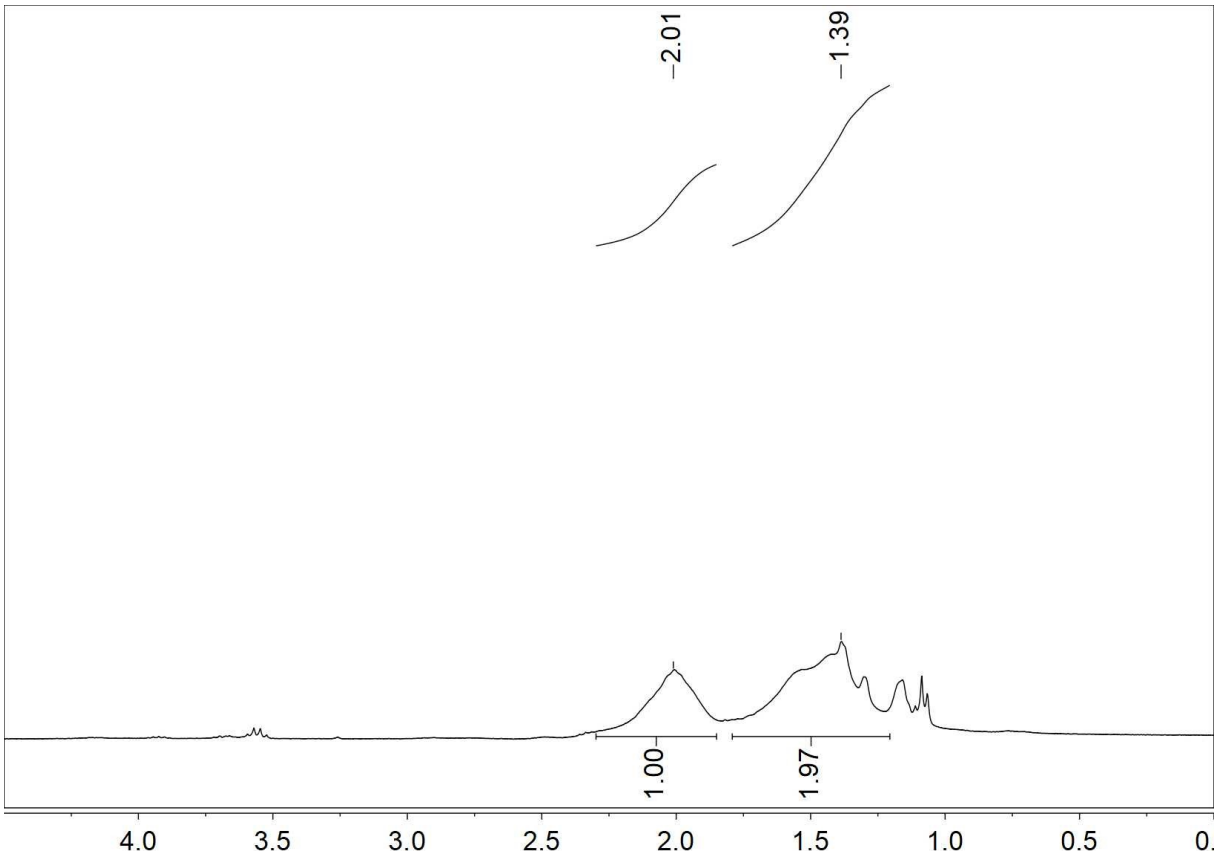

Figure S6. | ^{1}H NMR Spectra (D_2O) of PAANa with the numbers of hydrogen atoms determined by integration of the peak areas.

Figure. S7.

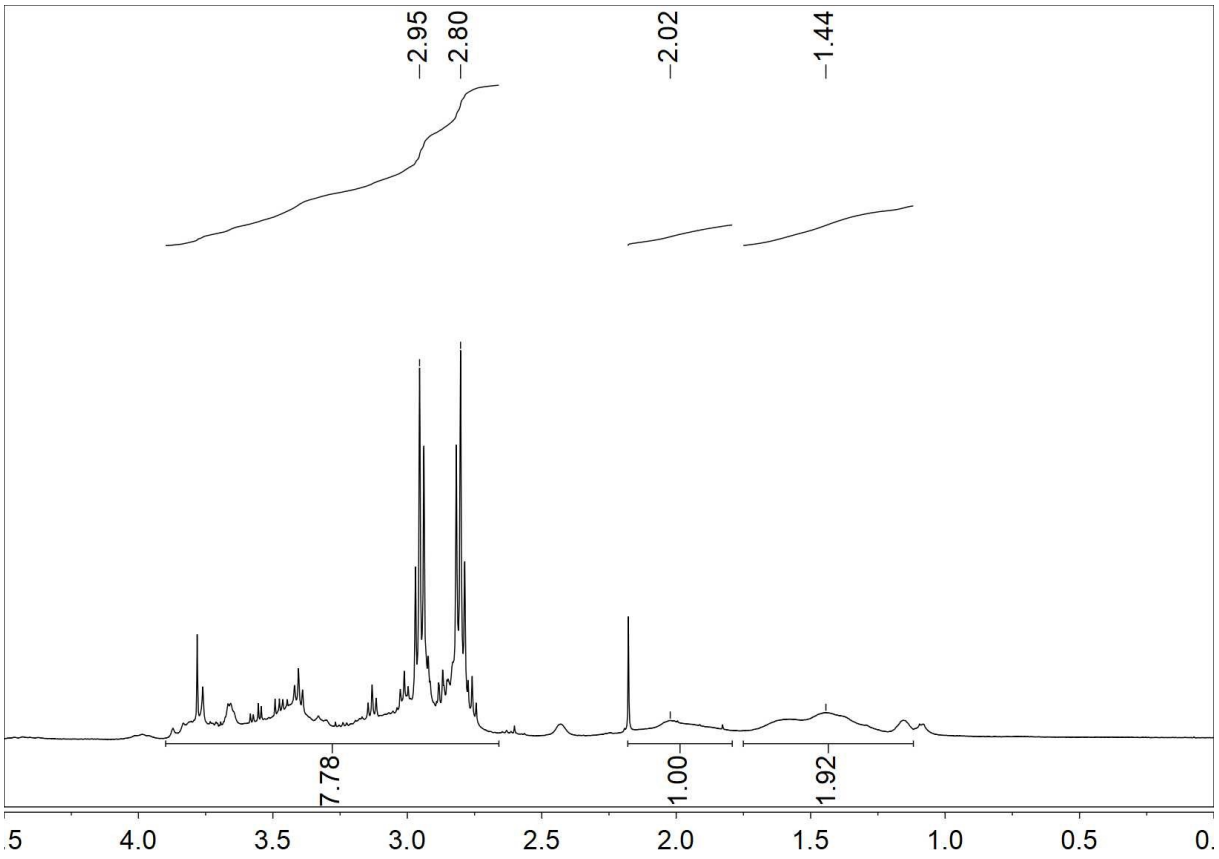

Figure S7. | ^{1}H NMR Spectra (D_2O) of PAA-DET. Calculated by comparing the PAANa backbone signals with the diethylenetriamine signals, within NMR error, approximately 52 of the 54 carboxyl groups on the PAANa side chain are attached to DET.

Figure. S8.

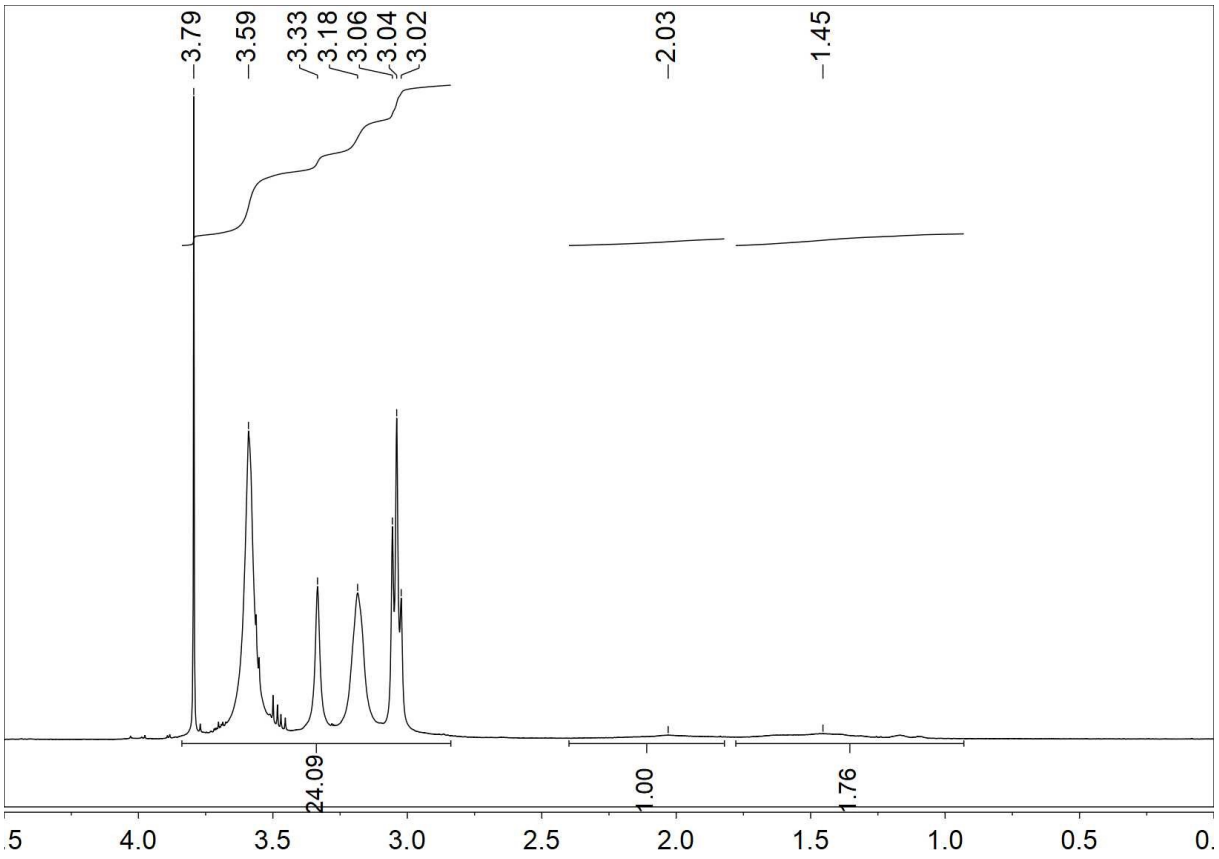

Figure S8. | ^{1}H NMR Spectra (D_2O) of PAA-DTPA. Calculations by comparing the PAANa backbone signals with the diethylenetriaminepentaacetic acid signal show that approximately 48 of these 52 $–NH_2$ were further coupled to DTPA.

Figure S9.

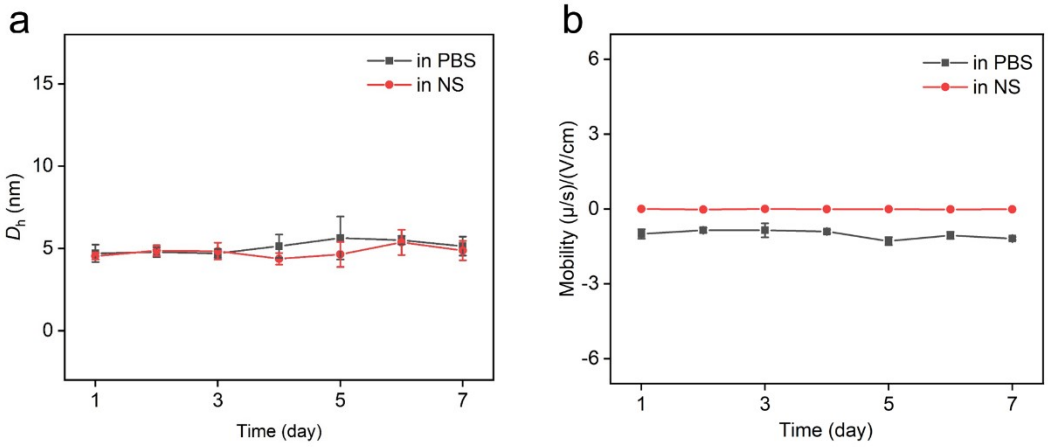

Figure S9. | Temporal evolutions of (**a**) the hydrodynamic size and (**b**) the electrophoretic mobility of PAA-Gd in PBS or NS.

Movie S1.

Supplementary Video 1. | Contralateral renal to ISI injection site

Movie S2.

Supplementary Video 2. | Ipsilateral renal to ISI injection site

Movie S3.

Supplementary Video 3. | Interstitial stream pathway

Movie S4.

Supplementary Video 4. | Lymphangiography versus interstitial stream imaging using intravital microscopy *in vivo*

Movie S5.

Supplementary Video 5. | Video of IVI with PAA-Gd using intravital microscopy *in vivo*

Code S1.

Supplementary Code 1. | Code to calculate relaxivity in Figure 1.g.

Code S2.

Supplementary Code 2. | Code to calculate T1 values using multi-FA in Figure 1.g.

Code S3.

Supplementary Code 3. | Code to analysis the signal intensity along time course in Figure 2.c.

Code S4.

Supplementary Code 4. | Code to valuate the RGB scatter in histochemical staining slice sections in Figure S2.k.

Experimental Section/ Materials and Methods

1. Chemical reagents and materials.

Gadolinium (III) chloride hexahydrate ($GdCl_3 \cdot 6H_2O$, 99.9%), sodium polyacrylate (PAANa, Mw = 5000), diethylenetriamine (DET), diethylenetriaminepentaacetic acid (DTPA), 4-(4,6-dimethoxy-1,3,5-triazin-2-yl)-4-methyl morpholinium chloride (DMTMM), and Chlorophosphonazo III (CPN III) were purchased from Aladdin Co. Ltd. (Shanghai, China). Sodium hydroxide (NaOH, 96%), sodium bicarbonate ($NaHCO_3$), and sodium citrate were obtained from Beijing Chemical Reagents Co. Ltd. (Beijing, China).

2. Synthesis of PAA-DET polymer.

PAA (120 mg) was dissolved in 12 mL Milli-Q water through magnetic stirring in a round-bottomed flask, and DET (1.1 mL) was subsequently added, followed by the immediate addition of DMTMM (1.152 g dissolved in 21 mL 0.01 M $NaHCO_3$ solution). This mixture was then stirred overnight at room temperature (RT at 21℃) and purified using 3k MWCO centrifugal devices to remove the unreacted DET molecules and to neutralise pH (2000 r/min for 3 times). The PAA-DET polymer was obtained as a white solid after freeze-drying.

3. Introduction of pendant DTPA groups to form PAA-DTPA.

DTPA (8 g) was dissolved in 11.4 mL Milli-Q water in a flask, and its pH was adjusted to 8.5 through the addition of 5 M NaOH. Next, the DMTMM (1.5 g) was added rapidly, and the mixture was stirred for 10 min at RT to activate one of the carboxyl groups in each DTPA. Next, prepared PAA-DET was added to cause reaction with activated DTPA for 4 h and form PAA-DTPA. A white product was obtained after purifying through 3k MWCO centrifugal devices and freeze-drying.

4. Coordination of Gd^{3+} to construct the PAA-Gd contrast agent.

Here, 30 mg PAA-DTPA synthesised in the previous step and $GdCl_3 \cdot 6H_2O$ (60.2 mg) were dissolved in 2 mL and 3.24 mL citric acid and sodium citrate buffer solution, respectively. Next, the Gd^{3+}-containing solution was dripped slowly into the PAA-DTPA solution and stirred at low speeds for 3 h. Next, 3k MWCO centrifugal devices were used to remove free Gd^{3+} ions and convert the solvent to 1 × PBS. The product was stored at 4 °C.

5. PAA-Gd Characterisation.

The products obtained at each step were characterised by ^1H NMR and dynamic light scattering (DLS) (Malvern Zetasizer Nano ZSE, the United

Kingdom) was used to measure the hydration particle size and electrophoretic mobility of as-prepared samples.

6. MRI characters of PAA-Gd agent.

The relaxivity measurements were carried out on a 1.5 T clinical MRI instrument (iSpace Pro 1.5 T, Beijing Wandong Medical Technology Co., Ltd., Beijing, China). A series of aqueous solutions of PAA-Gd and Gd-DPTA in 2.0 mL Eppendorf tubes were prepared. The content of Gd^{3+} in each tube was: 0, 0.025, 0.05, 0.10, 0.25, 0.50, 0.75, and 1.00 mM. The scanning parameters of the 2D-Fast Gradient Recalled Echo sequence were set as follows: TE=10 ms, TR=80 ms, and NEX=4; the FA were set as 7°, 10°, 12°, 15°, 17°, 20°, 25°, 30°, 35°, 40°, 45°, 50°, 55°, 60°, 65°, 70°, 75°, 80°, 85°, and 90° to gain flip angle-dependent signal images to acquire a T_1 relaxation time map.

The increase in the inverse of the T_1 relaxation time is linearly related to the constant of proportionality, namely, the longitudinal relaxivity (r_1) of the T_1-shortening agent or the concentration (C) of the MRI agent in the solution or tissue as follows:

$$\frac{1}{T_1} = \frac{1}{T_{1,0}} + r_1 \cdot C \quad , \tag{1}$$

where $T_{1,0}$ refers to the transverse relation time before the agent, namely the T_1 of pure de-ionised water in the phantom test.

For all matter (material or biological tissues) with certain T_1 and T_2 as constants, MRI parameters such as TR and TE determined the signal intensity of each, expressed as follows [1]:

$$S_{(\alpha)}^{S.S.} = M_0 \left(\frac{1 - e^{-TR/T_1}}{1 - e^{-TR/T_1} \cos \alpha} \right) e^{-TE/T_2} \sin \alpha \quad , \tag{2}$$

where M_0 refers to the proton density. For T_1 weighted images, the decrease in T_1 enhanced the signal intensity under the same MRI acquisition protocols. With a certain range of $T_{1,0}$ to T_1 over the time ($T_{1,t}$) after agent injection, the signal intensity increased, as displayed in Equation (2), with a sharp decrease in the relaxation time [Equation (1)].

For DCE applied with the gradient echo sequence to acquire T_1 weighted images with multiple repetitions, the signal intensity is expressed as follows:

$$SI_0^{'} = M'\left(\frac{1 - e^{-TR/T_1}}{1 - e^{-TR/T_1}\cos\alpha}\right)\sin\alpha \quad , \tag{3}$$

where α refers to the FA.

The Ernst angle (α_E), at which the MRI signal is maximised, can be calculated as follows:

$$\alpha_E = \arccos\left(e^{-TR/T_1}\right), \tag{4}$$

where T_1 refers to the longitudinal relaxation value of a particular tissue.[2] The T_1 mapping of PAA-Gd and DTPA-Gd were polyfitted according to Equation (2), and the longitudinal relaxivity, r_1, is calculated according to Equation (1) using first-order polynomial curve fitting. The theoretical Ernst angle was calculated according to the scanning condition when TR is large enough that it cannot be ignored, the T_1 value of tissue post-enhancement decreases dramatically, and the α_E reaches a limit of 45° according to Equation (4). The analysis and calculations were performed using MATLAB R2016a (The MathWorks Inc., Natick, Massachusetts, USA).

7. Cytotoxicity of the PAA-Gd agent.

HUVEC was cultured in an EGM-2 medium (Lonza, Visp, Switzerland) with a 2% foetal bovine serum and vascular endothelial growth factor, supplied in EGM-2 BulletKit (CC-3162) under 5% CO_2 atmosphere at 37 °C.

Cytotoxicity was assessed on HUVEC by using the WST-8 solution (Sigma Cell Counting Kit 8, Dojindo Laboratories, Japan). Exponentially growing HUVEC was seeded on 96-well plates at a density of 5×10^3 cells per well. After 36 h incubation at 5% CO_2 and 37 °C, the medium was replaced with diluted PAA-Gd and Gd-DTPA at a range of concentrations (0, 0.03, 0.06, 0.12, 0.20, 0.25, and 0.5 mM) and then incubated for 12 h. Cell viability was assayed by the addition of WST-8 into the 96-well plates. Subsequently, the optical density at 450 nm was measured after 3 h.

8. *In vivo* MR imaging.

Eight-week-old male BALB/C mice (n=6, 18–20 g body weight) were obtained from Beijing Vital River Experimental Animal Corporation (Beijing, China). All animal study procedures were performed under the supervision of the Ethics Committee at the National Center for Nanoscience and Technology and in compliance with the handling guidelines and protocols for use, maintenance, and care of laboratory animals (ID: NCNST21-2011-0612). For MRI in vivo imaging, the mice were settled in a 7 Tesla MR scanner (Biospec

70/20 USR, Bruker, Germany) with a mono-tunnelled birdcage coil. The animals were anesthetised for fixation. During the indwelling needle setting and image acquiring process, 3% isoflurane anaesthesia was delivered through the nose and oral cavity using a gas duct. The experiments were done at the room temperature of 21°C.

T_1- weighted spin echo [500/30/2 (TR/TE/Average)] and T_2- weighted fast spin-echo [3000/100/2 (TR/TE/Average)] were adapted before agent injection. DCE images were acquired from pre-injection to approximately 30 min post-injection *in situ* continuously and comprised 2D T_1 weighted Fast Low Angle Shot (FLASH) images for a certain time course. The details of the sequence are as follows: bandwidth 20 wHz, field of view 100 mm × 50 mm, matrix size 256 × 128, 20 coronal slices, slice thickness 1 mm (no gap), TE = 1.68 ms, TR = 80.02 ms, FA = 45° (the theoretical Ernst angle discussed above), repetition = 250, and time resolution 7.68 s.

The PAA-Gd agent (100 μL, Gd concentration: 0.8 mg/mL) was suspended with the PBS solution and injected by using an indwelling needle in the tarsal tunnel formed by the medial malleolus of the tibia at the posteromedial side of the ankle through the ISI method [3, 4] during MR scanning. The IVI group was applied the same dosage and solution through intravascular injection, which was finished within 60 s. The image acquisition started 2 min ahead of agent injection and lasted for 10 to 30 min. Throughout the scanning process, the heart and the breath rate were monitored steadily, and the body temperature of the mice was kept at 37 °C. The ISI and IVI groups for which scanning was performed within 10 min were removed from histological investigation and ICP-MS.

The *in situ* quantitative analysis of paravascular space was done in the selected ROI. The region was manually drawn at the time of the highest signal intensity, and the mask was created to multiply with all images during a DCE scanning in the certain slice section as shown in **Figure 2b**.

9. Quantitative analysis of gadolinium.

ICP-MS was used to quantitatively measure the absolute mass of gadolinium in various tissues. Animals were sacrificed within six to eight minutes after ISI and IVI injection (in two assigned groups) and the MRI study. The experiments were done at the room temperature of 21°C.The subcutaneous injection group was added to experimental research on ICP-MS for comparison. The dosage and concentration used in the subcutaneous injection of PAA-Gd on animals were maintained the same for the ISI and IVI groups.

The blood was collected by removing the eyeball. The veins were ligated to prevent fluid moiling. The sutures were seamed at the edge of the bilateral femoral vein, renal vein and abdominal aorta.

The blood vessels were sampled with vascular membrane, and the sections collected were listed and numbered as follows: (1) blood sample, (2) ipsilateral femoral vein of injection, (3) heterolateral femoral vein of injection, (4) abdominal aorta of injection, (5) heterolateral renal vein of injection, (6) ipsilateral renal vein of injection, (7) mesentery. The samples were then digested using wet digestion. The heating table was filled evenly with sea sand and fixed with tinfoil, and the serum bottles were inserted into the sea sand so that the upper surface of the liquid in the bottle was even or lower than the surface of the sea sand. Two to three drops of hydrogen peroxide solution were added into the bottles and the samples were heated to 80 °C on the heating table. Next, the bubbles were created with continued heating to 140 °C and slow addition of hydrogen peroxide (1.42 g/mL) at a speed of 2–3 drops/min.

The solution was steam-dried to a drop of concentrated solution and then diluted with a 1% HNO_3 before getting transferred to a centrifugal tube at a constant volume. The constant volume solution consisted of 1% HNO_3 and 1% HCl solutions.

Standard liquid containing a certain amount of gadolinium element was prepared using the same volume liquid, and the standard curve was drawn. The mass of gadolinium in the original sample was calculated as follows:

$$\Omega = \frac{(\rho - \rho_0) \cdot V \cdot f}{m} \quad (5)$$

In the equation, ρ and ρ_0 represent the concentrations of gadolinium in the sample and blank, respectively, and V represents the volume of the liquid after tissue digestion and re-dissolving. The mass calculated from Equation (5) was divided by the mass of gadolinium in the blood sample, and its relative content in the tissues was recorded. According to the definition, the relative gadolinium content in the blood sample was one.

10. Histological study.

Tissue fixation before the histochemical study was performed six to eight min after injection when two groups of mice were sacrificed. Kidney tissue was collected, fixed with paraformaldehyde (4% w/v), embedded with paraffin, and sliced with coronal sections, and subsequently deparaffinised and hydrated. The sections were stained with Haematoxylin and Eosin Y (H&E), Masson trichrome dyes, and CPN III.[5] The images of stained tissues (**Figure 3g-h**,

Figure 5d-g) were obtained with digital slide scanner NanoZoomer S210 (Hamamatsu Photonics Ltd., Hamamatsu City, Japan). The slides were imaged under the same calibrated light density conditions as in the slide cassette.

11. Intravital microscopy *in vivo* imaging.

The PAA-Gd agent (100 μL, Gd concentration: 1.0 mg/mL) was suspended with the PBS solution and injected by using an 1ml clinical syringe in the tarsal tunnel formed by the medial malleolus of the tibia at the posteromedial side of the ankle on the left leg through the ISI method. Evan's Blue dye was injected into the medial site under skin near vein (VGS) of the left leg. The CPN III was slowly dripped on the surface of surgery section after the skin was removed till the surface was wholly immerse with CPN III solution. IVI injected group (at VGS) was done as the identical protocols as above. Images and videos were acquired by an intravital microscopy 5 min after injection (**Supplementary Movie 4** and **Supplementary Movie 5**). The experiments were done at the room temperature of 21°C.

12. Statistical analysis.

The images collected from the slide scanner without further processing were presented with NDP viewer2 (Hamamatsu Photonics Ltd., Hamamatsu City, Japan). The RGB analysis, presented using Origin 7.0 (OriginLab Corp., Northampton, Massachusetts, USA), was performed on a kidney slice (1.5×) stained with CPN III, and the data analysis was performed using MATLAB R2016a (The MathWorks Inc., Natick, Massachusetts, USA). Codes are available in the Supplementary Materials.

References

1. R. W. Brown, Y.-C. N. Cheng, E. M. Haacke, M. R. Thompson and R. Venkatesan, *Magnetic resonance imaging: physical principles and sequence design*, John Wiley & Sons, 2014.
2. R. R. Ernst and W. A. Anderson, *Review of Scientific Instruments*, 1966, **37**, 93-102.
3. X. Shi, Y. Zhu, W. Hua, Y. Ji, Q. Ha, X. Han, Y. Liu, J. Gao, Q. Zhang and S. Liu, *Nano Research*, 2016, **9**, 2097-2109.
4. H.-y. Li, M. Chen, J.-f. Yang, C.-q. Yang, L. Xu, F. Wang, J.-b. Tong, Y. Lv and C. Suonan, 2012.
5. J. Huang, Y. Hou, T. Ma, P. Zhang, Y. Li, C. Liu, B. Zhang, S. Qiu, J. Zeng and M. Gao, *Advanced Therapeutics*, 2018, **1**, 1800005.